CERN-INTC-2020-036 / INTC-P-561
13/05/2020

EUROPEAN ORGANIZATION FOR NUCLEAR RESEARCH

Proposal to the ISOLDE and Neutron Time-of-Flight Committee

Laser spectroscopy of neutron-rich tellurium isotopes

May 13, 2020

L. V. Rodríguez[1], S. Bai[2], M. L. Bissell[3], K. Blaum[1] B. Cheal[4], R. F. García Ruíz[5], H. Heylen[6], A. Kanellakopoulos[9], J. Kraemer[7], T. Lelligner[7], S. Malbrunot-Ettenauer[6], R. Neugart[1,8], G. Neyens[6,9], W. Nörtershäuser[7], R. Sánchez[10], X. Yang[2], D. T. Yordanov[11]

[1]*Max-Planck-Institut für Kernphysik, Heidelberg, Germany.*
[2]*School of Physics and State Key Laboratory of Nuclear Physics and Technology, Peking University, Beijing, China*
[3]*School of Physics and Astronomy, The University of Manchester, Manchester, United Kingdom*
[4]*Oliver Lodge Laboratory, University of Liverpool, United Kingdom*
[5]*Massachusetts Institute of Technology, Cambridge, MA, USA*
[6]*Experimental Physics Department, CERN, Geneva, Switzerland*
[7]*Institut für Kernphysik, Technische Universität Darmstadt, Darmstadt, Germany*
[8]*Institut für Kernchemie, Universität Mainz, Mainz, Germany*
[9]*Instituut voor Kern- en Stralingsfysica, KU Leuven, Leuven, Belgium*
[10]*GSI Helmholtzzentrum für Schwerionenforschung GmbH, Darmstadt, Germany*
[11]*Université Paris-Saclay, CNRS/IN2P3, IJCLab, 91405 Orsay, France*

Spokesperson: L. V. Rodríguez, liss.vazquez.rodriguez@cern.ch
Contact person: L. V. Rodríguez, liss.vazquez.rodriguez@cern.ch

Abstract:

This proposal aims to study the neutron-rich tellurium isotopes $^{112-137}$Te, having two protons outside the $Z = 50$ shell, by high-resolution laser spectroscopy. The goal is the determination of spins, electromagnetic moments and charge radii from the hyperfine structures and isotope shifts, which will contribute to a better understanding of the nuclear structure in the vicinity of the doubly-magic ^{132}Sn. One particular question we want to address, is whether the two protons outside of the tin core have the same polarizing effect on the quadrupole moments of the $11/2^{-}$ states, as the two proton holes in cadmium.

Requested shifts: 18 shifts (1 run)

1 Introduction

Nuclei near closed shells are of great interest for both experimental and theoretical nuclear-structure investigations. With two protons above the $Z = 50$ shell closure, the tellurium isotopes are such an example. Several studies, including laser spectroscopy, have been devoted to measurements of the electromagnetic properties of ground and isomeric states of $^{119-135}$Te [1–4]. An overview of the existing data is summarized in Table 1. For the magnetic moments, an almost complete dataset is available. However, the data obtained with laser spectroscopy [1] have rather large error bars. Thus more precise and accurate magnetic moments will help to unravel details about the purity of the nuclear wave functions as a function of neutron number. For the quadrupole moments, relatively few are known and the error bars are very large such that little nuclear structure conclusions can be made.

Table 1: Literature values for the magnetic and quadrupole moments of ground- and isomeric states of tellurium isotopes. The abbreviation of methods are as following; AB: Atomic beam magnetic resonance; NMR/ON: Nuclear magnetic resonance on oriented nuclei; NMR: Nuclear magnetic resonance; LS: Laser spectroscopy; NO/ME: Mössbauer effect on oriented nuclei.

	I^π	$T_{1/2}$	$\mu(\mu_N)$	method	Q(b)	method
^{119g}Te	$1/2^+$	16.05 h	0.25(5)	AB		
^{119m}Te	$11/2^-$	4.70 d	0.894(6)	NMR/ON		
^{121g}Te	$1/2^+$	19.17 d				
^{121m}Te	$11/2^-$	164 d	0.895(10)	NMR/ON		
^{123g}Te	$1/2^+$	9.2×10^{16} y	−0.7358(3)	NMR		
^{123m}Te	$11/2^-$	119.2 d	−0.927(8)	NMR/ON		
^{125g}Te	$1/2^+$	stable	−0.8885051(4)	NMR		
^{125m}Te	$11/2^-$	57.4 d	−0.985(6)	NMR/ON	0.0(2)	LS
^{127g}Te	$3/2^+$	9.35 h	0.635(4)	NMR/ON		
^{127m}Te	$11/2^-$	106.1 d	−1.041(6)	NMR/ON	+0.17(12)	LS
^{129g}Te	$3/2^+$	69.6 m	0.702(4)	NMR/ON	0.055(13)	NO/ME
^{129m}Te	$11/2^-$	33.6 d	−1.091(7)	NMR/ON	+0.4(3)	LS
^{131g}Te	$3/2^+$	25.0 m	0.696(9)	NMR/ON		
^{131m}Te	$11/2^-$	33.25 h	−1.123(7)	NMR/ON	+0.25(14)	LS
^{133g}Te	$3/2^+$	12.5 m	+0.85(2)	LS	+0.23(9)	LS
^{133m}Te	$11/2^-$	55.4 m	−1.129(7)	NMR/ON	+0.28(14)	LS
^{135g}Te	$7/2^-$	19.0 s	−0.69(5)	LS	+0.29(9)	LS

With the expected yields from ISOLDE, associated with a recently developed RILIS ionization scheme for tellurium [5], collinear laser spectroscopy will provide high-resolution

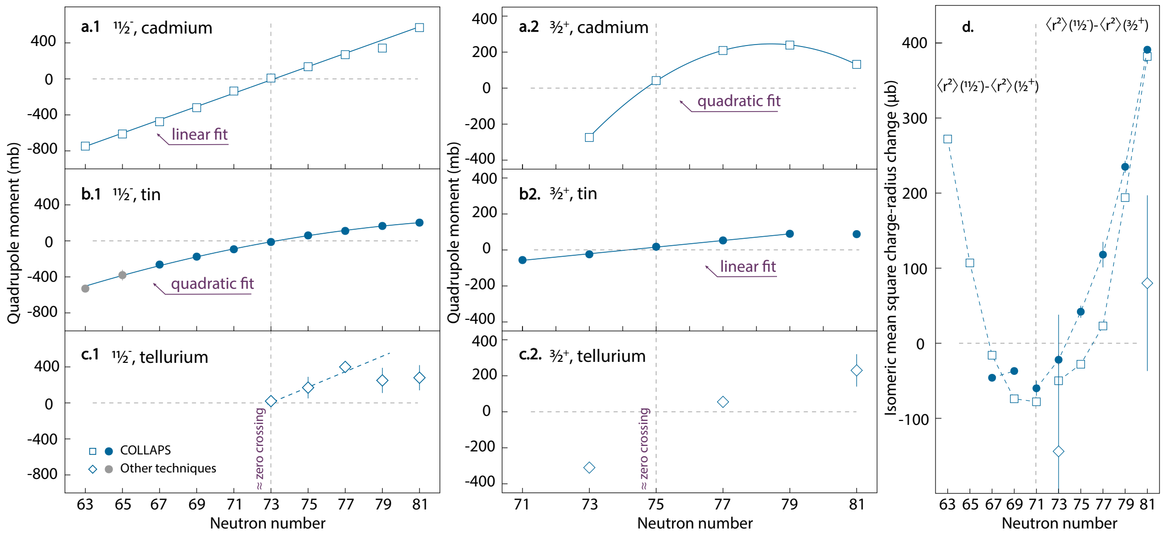

Figure 1: Quadrupole moments of $11/2^-$ and $3/2^+$ states in **a.** cadmiun ($Z = 48$), **b.** tin ($Z = 50$) and **c.** tellurium ($Z = 52$). **d.** Mean square charge-radii changes for the $11/2^-$ states relative to the $1/2^+$ and $3/2^+$ states. The data are taken from Refs. [1, 6, 7]

data in the range $112 \leq A \geq 137$. Within this range, a series of particular isotopes are key for the physics case of this proposal as discussed below.

2 Physics case

2.1 Simple patterns in complex nuclei

The COLLAPS experiment has yielded a wealth of new information about moments and charge radii of long isotopic sequences in the region of the doubly-magic nucleus ^{132}Sn. This allowed the investigation of interesting phenomena which appear as regularities in the measured trend. In particular, we have shown that the quadrupole moments of the $11/2^-$ and $3/2^+$ states in cadmium ($Z = 48$) and tin ($Z = 50$) exhibit a simple linear or quadratic behavior with increasing neutron number [6, 7]. The experimental results are displayed in Fig. 1, insets a and b. While common patterns are perceived for both isotopic chains, e.g. the trends change from negative to positive with a nearly zero value at $N = 73$ in the $11/2^-$ states and at $N = 75$ in the $3/2^+$ states, a significant attenuation of the quadrupole moments is observed in the closed-shell tin with respect to those in cadmium, which quantifies the impact of the proton-hole pair (in Cd). On the other hand, mean square charge-radii were found to exhibit a parabolic behaviour with changing neutron number, as shown in Fig. 1d, and surprisingly, to be of similar strength in both isotopic chains even though the quadrupole moments are considerably reduced in tin. With aim to investigate these behaviours as a function of the proton number, we propose to study the tellurium chain, having two protons above the closed shell in tin, as opposed to the two proton holes in cadmium.
The existing data on the relevant states in tellurium are shown in Fig. 1, insets c and

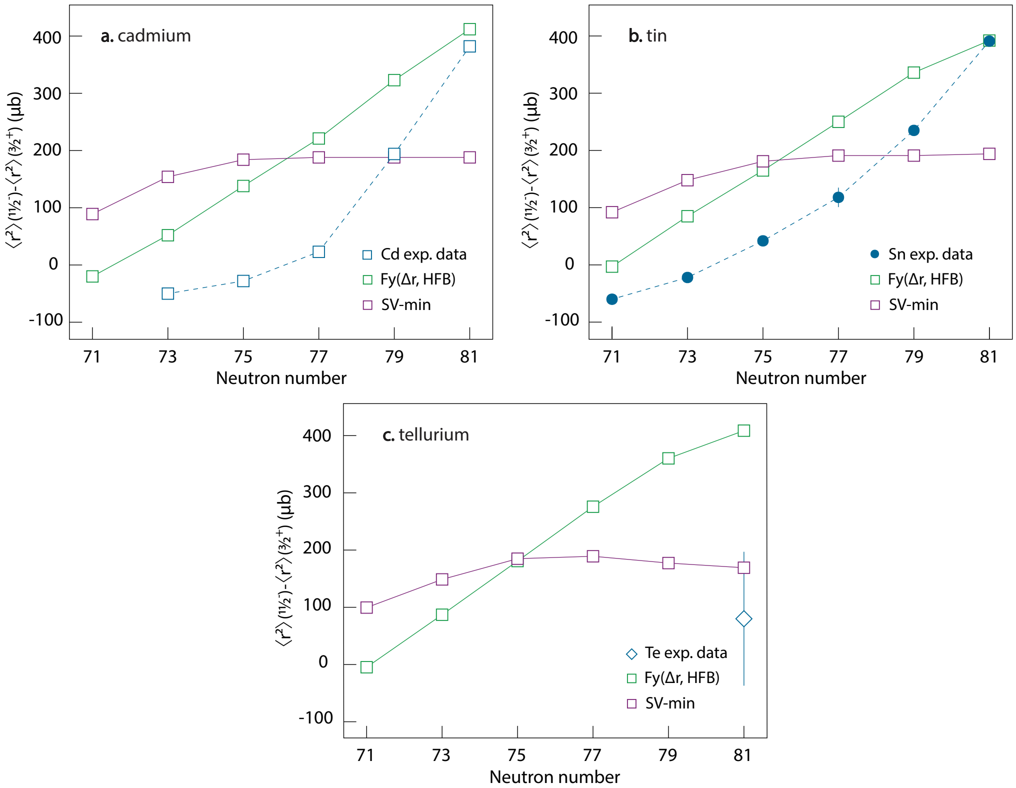

Figure 2: Experimental and theoretical isomeric mean square charge-radii changes for the $11/2^-$ states relative to the $3/2^+$ states in **a.** cadmium, **b.** tin and **c.** tellurium obtained with SV-min and the Fayans Fy(Δr, HFB) functional [18].

d. So far only five quadrupole moments of $11/2^-$ states were measured and have very large uncertainties. Three out of these five seem to support a similar linear trend with a zero crossing at $N = 73$, but the other two clearly deviate from this behaviour, even when considering the rather large error bars. We have to note that also in the case of tin, deviations of previously reported values beyond their uncertainties were found in the COLLAPS measurements, revealing the smooth behavior that was not obvious in the old data. Apart from confirming this linear trend over a long chain of Te isotopes, it will be interesting to investigate whether the polarizing effect of two proton holes (in Cd) is the same as that of two proton particles (in Te).
Compared to the $11/2^-$ states, the available data for the mean square charge-radii changes in tellurium are scarce and inconclusive. However, if we look at $N = 81$ the experimental value in tellurium is four times smaller than in tin and cadmium. Mean square charge-radii changes were calculated for the tellurium species [9] using two different DFT functionals, Skyrme SV-min and Fayans Fy(Δr), also employed in the interpretation of our previous work on Cd and Sn isotopes [7]. In Fig. 2, the theoretical results are compared to the experimental data. One can see that both functionals predict similar patterns for the three cases. However, the SV-min agrees with the experimental value in tellurium, while it is the Fy(Δr) that stays closest to the cadmium and tin data. Measurements of the mean

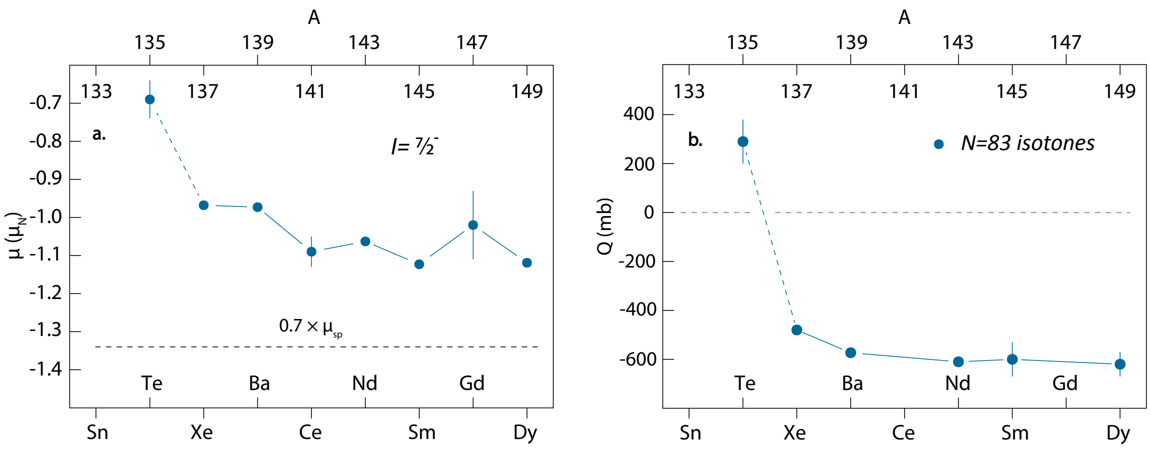

Figure 3: **a.** Magnetic and **b.** quadrupole moments of $N = 83$ isotones with even Z up to $Z = 66$. The dashed black line in **a.** represents the single-particle Schmidt value. Experimental values are taken from [1, 10–17].

square charge-radii changes in Te with high-resolution will help to benchmark nuclear theory in this region.
For these reasons, we propose to measure the quadrupole moments and mean square charge-radii changes of $^{115-133}$Te with high-resolution.

2.2 Electromagnetic moments of $N = 83$ isotones

In Fig. 3, the magnetic and quadrupole moments of $N = 83$ isotones with even Z up to $Z = 66$ are shown. All magnetic moments are rather similar except for ^{135}Te, while its quadrupole moment is reported with a sign opposite to the expectations from the systematics. Particularly, this is in contradiction with our recent measurement of the electromagnetic moments in ^{133}Sn [23]. Realistic shell-model calculations do not support the values of tellurium while reproducing the experimental data of other $N = 83$ isotones [23]. For these reasons, we propose to address the electromagnetic moments of ^{135}Te in high resolution, in order to unravel the underlined nuclear structure. Furthermore, such a measurement will contribute to a better understanding of the ^{132}Sn region.

3 Experiment

The ground- and isomeric-state properties of $^{112-137}$Te will be determined from the hyperfine structures and isotope shifts measured via optically detected laser spectroscopy at the COLLAPS setup. The beam delivered by ISOLDE will be accumulated in the radio-frequency Paul trap ISCOOL [20], transported as short bunches to the collinear-beam apparatus, post-accelerated and neutralized by charge-exchange with potassium vapour [21, 22]. A continuous-wave laser beam will be collinearly superimposed with the bunched atomic beam and the fluorescence photons will be detected using four photomultiplier tubes. The background count rate will be suppressed by gating on the pulsed

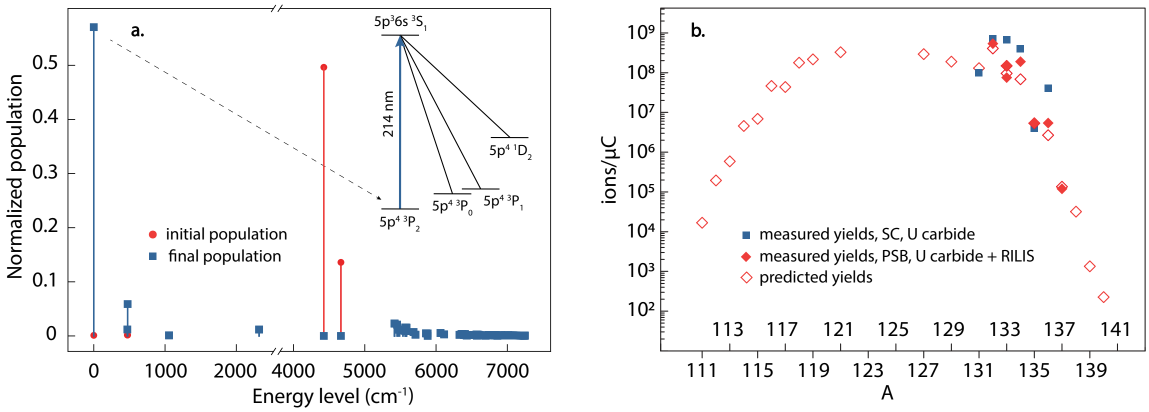

Figure 4: a. Simulations of the atomic population distribution of a 40-keV ionic tellurium beam following neutralisation by potassium vapour. Red circles and blue squares represent the initial population after charge exchange at 0-cm and the final population after a further 40-cm of atom flight, respectively. b. Measured and predicted yields of tellurium isotopes.

beam structure. Details concerning the experimental set-up can be found in the review by Neugart et al. [24].
We propose to perform the spectroscopy on the $5p^4\ ^3P_2 \rightarrow 5p^3 6s\ ^3S_1$ transition in the neutral atom, which is highly sensitive to the nuclear electromagnetic properties. The atomic ground state is expected to be favored in the charge exchange process, accumulating more than 50 % of the total population. This is shown in Fig. 4a where simulations of the atomic population distribution of a 40-keV ionic tellurium beam following neutralisation by potassium vapour are presented [25]. The 214 nm wavelength will be produced by a titanium-sapphire laser, pumped at 532 nm and coupled to two external cavities to quadruple the output laser frequency.
Tellurium beams will be produced by a uranium carbide target and laser ionized in a hot cavity. The production yields associated to this type of target have been measured with primary beam from the CERN synchrocyclotron (SC) [26] as well as from the proton synchrotron booster (PSB) [27]. The measured values are plotted in Fig. 4b together with the prediction for the remaining cases. Cesium isobars are expected to be the dominant contaminants in neutron-rich beams, therefore, the use of a "neutron converter" [28] is required. This will influence the production rates shown in Fig. 4b, which will drop by a factor from 3 to 10 while alkali contaminants will be suppressed by a factor from 10 to 100. The experience that we gained with bunched beams leads us to consider a sensitivity limit of laser spectroscopy experiments of 10^4 ions/μC at COLLAPS [30], therefore, it is feasible to perform the spectroscopy from $A = 112$ to $A = 137$.

4 Beam-time request

Typical times for measuring the hyperfine structures are: 0.5 shift for isotopes with yields greater than 10^5 ions/μC and 1 shift for isotopes with yields equal or less than that. Since there are 26 isotopes that can be measured and about half of them have an isomeric state, we request 16 shifts of radioactive beam using a UC_x target, RILIS, HRS and ISCOOL, one shift of stable beam before the experiment, and one shift for RILIS setup, these 18 shifts in total preferred in one run.

Summary of requested shifts: One experiment of 17 shifts of radioactive beam and 1 shift of stable beam are requested for the study of the tellurium isotopes $^{112-137}$Te.

References

[1] R. Sifi *et al.*, Hyp. Interact. **171**, 173 (2006).

[2] S. Vajda *et al.*, Phys. Lett. B **42**, 54 (1972).

[3] K. Nishimura, S. Ohya and N. Mutsuro, Phys. Rev. C **36**, 2069 (1987).

[4] R.Geerts *et al.*, Phys. Rev. C **21**, 439 (1980).

[5] T. Day Goodacre *et al.*, Nucl. Instrum. Methods Phys. Res., Sect. A **830**, 510 (2016).

[6] D.T. Yordanov *et al.*, Phys. Rev. Lett **110**, 192501 (2013).

[7] D.T. Yordanov, L. V. Rodríguez *et al.*, Comm. Phys (2020).

[8] P. W. Zhao, S. Q. Zhang, J. Meng *et al.*, Phys. Rev. C **89**, 011301 (2014).

[9] P-G. Reinhard, W. Nazarewicz, Private communication (2020).

[10] W. Borchers *et al.*, Phys. Lett. B **216**, 7 (1989).

[11] K. Wendt, S. A. Ahmad, C. Ekström *et al.*, Z Phys. A **329**, 407 (1988).

[12] W. an Rijswijk *et al.*, Hyp. Interact. **15**, 325 (1983).

[13] K. F. Smith and P. J. Unsworth, Proceedings of the Physical Society **86**, 1249 (1965).

[14] P. Aufmuth, A. Bernard and M. Deckwer *et al.*, , Z Phys. D **23**, 19 (1992).

[15] J. G. England *et al.*, J. Phys. G **16**, 105 (1990).

[16] T. I. Kracikova, S. Davaa and M. Finger, Hyp. Interact. **34**, 69 (1987).

[17] D. A. Bromley, Treatise on Heavy Ion Science, Boston, 978-1-4613-0713-6 (1989).

[18] S. A. Fayans *et al.*, JETP Lett. **68**, 169 (1998).

[19] J. M. Allmond *et al.*, Phys. Rev. Lett **118**, 092503 (2017).

[20] E. Mané *et al.*, Eur. Phys. J. A **42**, 503 (2009).

[21] A. Mueller *et al.*, Nucl. Phys. A **403**, 234 (1983).

[22] A. Klose *et al.*, Nucl. Instr. Meth. Phys. Res. A **678**, 114 (2012).

[23] L. V. Rodríguez *et al.*, in preparation.

[24] R. Neugart *et al.*, J. Phys. G **44**, 064002 (2017).

[25] A. Vernon *et al.*, Spectrochim. Acta B, **153**, 61 (2019).

[26] H.-J. Kluge (editor) ISOLDE Guide for Users; CERN 86-05 (1986).

[27] S. Rothe, Private communication (2020).

[28] R. Catherall *et al.*, Nucl. Instr. Meth. Phys. Res., Sec. B **204**, 235 (2003).

[29] U. Koster *et al.*, Nucl. Instrum. Methods Phys. Res., Sect. B **266**, 4229 (2008).

[30] D. T. Yordanov *et al.*, NTC-P-271, CERN-INTC-2009-036 (19 Oct 2009).

Appendix

DESCRIPTION OF THE PROPOSED EXPERIMENT

The experimental setup comprises:

Part of the	Availability	Design and manufacturing
COLLAPS	☒ Existing	☒ To be used without any modification

HAZARDS GENERATED BY THE EXPERIMENT
Hazards named in the document relevant for the fixed COLLAPS installation.